Thermodynamic Control of Electron Transfer Rates in Multicentre Redox Proteins

Teresa Catarino*[a] and David L. Turner[b]

In the analysis of kinetic data from multicentre redox proteins, it is essential to distinguish between the observable macroscopic rate constants and the structurally relevant microscopic properties. This distinction is complicated by the existence of interactions between centres. The problem is illustrated by the case of two interacting redox centres and generalised for the analysis of stopped-flow kinetic data for the reduction of cytochrome c_3, in which four redox centres and at least one proteolytic centre are mutually interacting. It is shown that fast intramolecular electron transfer, which is typical of many multicentre redox proteins, and, where present, fast proton exchange, ensure that only N rate constants can be measured for a protein with N redox centres. The equations that relate the observable macroscopic rate constants to the microscopic rate constants of individual centres depend on a set of parameters that can be approximated by using the Marcus theory of electron transfer together with a set of reasonable assumptions. The results are tested by fitting experimental data for the reduction of cytochrome c_3 by sodium dithionite, including its pH dependence.

KEYWORDS:

cytochromes · electron transfer · heme proteins · kinetics · Marcus theory

Introduction

Many important biological processes depend upon small soluble proteins or large protein complexes, including transmembrane proteins, that possess multiple redox centres. These proteins participate in electron transfer (ET) reactions that are often involved in energy transduction and/or catalysis. Rates of ET between centres within multicentre proteins have been studied intensively,[1] by using methods such as laser flash photolysis, with the aim of understanding how the proteins function. However, ET between such proteins and their physiological partners is essential to cell metabolism.

In this work we propose a model for analysing the kinetics of ET between multicentre redox proteins and their electron donors or acceptors, with the aim of obtaining information on the kinetic properties of the individual redox centres. The model is applicable to situations in which intramolecular ET is much faster than intermolecular ET. Under these conditions, the distribution of electrons inside the multicentre protein is thermodynamically controlled and the complex kinetic scheme that involves all possible (microscopic) ET steps collapses into a simple mechanism of *N* consecutive (macroscopic) ET steps for a protein with *N* redox centres. The macroscopic rate constant of each step is the weighted average of the microscopic rate constants that participate in the step, and the weights are the respective fractional populations.

The Marcus theory[2] can be used to establish a relationship between the rate constants of each individual centre at different levels of global reduction, on the basis of the driving force for each microscopic ET reaction. In this way, it becomes possible to extract information on the kinetic behaviour of the individual centres. Two different sets of assumptions are discussed. In model 1, the redox centres are assumed to be intrinsically different with respect to binding affinity for the electron donor and ET parameters such as the reorganisation energy, but these parameters are assumed to be independent of the global redox state. Thus, only the driving force for each redox centre is allowed to change from one step to another. In model 2, the redox centres are assumed to be similar in all respects other than their microscopic redox potentials. However, these parameters are assumed to depend on the global redox state and are allowed to change from step to step. Each model therefore requires only one variable per redox centre, but both models require a detailed thermodynamic characterisation of the multicentre redox protein in order to analyse the kinetic behaviour of individual centres.

The kinetic models described here are illustrated with an application to the reduction of cytochrome c_3, a tetrahaem cytochrome isolated from *Desulfovibrio gigas*, by sodium dithionite. It is shown that the models are capable of describing the pH dependence of the kinetic traces on the basis of the

[a] *Dr. T. Catarino[+]*
Instituto de Tecnologia Química e Biológica
Universidade Nova de Lisboa
Rua da Quinta Grande, 6, Apt. 127, 2780 Oeiras (Portugal)
Fax: (351) 214428766
E-mail: catarino@itqb.unl.pt

[b] *Dr. D. L. Turner*
Department of Chemistry
University of Southampton
Southampton SO17 1BJ (UK)

[+] *Further address:*
Departamento de Química, Faculdade de Ciências e Tecnologia
Universidade Nova de Lisboa, Monte da Caparica (Portugal)

  1439-4227/01/02/06 $ 17.50+.50/0 CHEMBIOCHEM **2001**, 2, 416 – 424

change in the driving force due to the haem–proton interactions (redox-Bohr effects) characterised previously,[3] hence validating the assumptions used.

One important aspect concerning the use of dithionite as reducing agent is that the complicated equilibrium chemistry of sodium dithionite and bisulfite makes its effective midpoint redox potential dependent on pH and also on concentration.[4] However, when the SO_2^- radical is the actual reducing agent,[5] the midpoint potential of the SO_2/SO_2^- couple is all that is relevant for the calculation of the driving forces. This has a value of -0.3 V which does not depend on the dithionite concentration and is pH-independent above pH 2.[6] An excess of dithionite and the equilibrium reactions of SO_2 that follow electron transfer from SO_2^- to the protein acceptor still drives the reaction to completion even for redox centres with negative midpoint potentials, such as those of cytochrome c_3.

Results and Discussion

Kinetic modelling of multicentre redox proteins

The complete kinetic scheme for an ET reaction between a protein, P, and an electron donor, D, has to take into account at least the following steps: 1) complex formation, 2) electron transfer within the complex, and 3) complex dissociation, as shown in Scheme 1. For a multicentre redox protein interacting

$$P^{ox} + D^{red} \underset{k_{-1}}{\overset{k_{+1}}{\rightleftharpoons}} [P^{ox}\text{-}\,D^{red}] \underset{k_{-2}}{\overset{k_{+2}}{\rightleftharpoons}} [P^{red}\text{-}\,D^{ox}] \underset{k_{-3}}{\overset{k_{+3}}{\rightleftharpoons}} P^{red} + D^{ox}$$

Scheme 1. *Kinetic steps for electron transfer with complex formation; P^{ox} and P^{red} represent the oxidised and the reduced states, respectively, of the protein, and D^{red} and D^{ox} represent the reduced and the oxidised states, respectively, of the electron donor. The complexes that result from the association of the redox partners are represented in brackets.*

with a single electron donor, this sequence of events should be considered for each individual centre. Since at least six rate constants are required for each redox centre, it is virtually impossible to define all of them. However, the analysis of the system can be simplified significantly with certain approximations, making it possible to determine rate constants that can be related to the rate constants of Scheme 1. In particular, under steady-state conditions, the complete kinetic scheme for the reduction of centre *i* in protein P can be approximated by a simple collisional model (Scheme 2). The rate constants

$$P_i^{ox} + D^{red} \underset{k_{-i}}{\overset{k_{+i}}{\rightleftharpoons}} P_i^{red} + D^{ox}$$

Scheme 2. *Rate constants for electron transfer in a simple collisional model.*

k_{+i} and k_{-i} in Scheme 2 are composite parameters, defined in Equations (1a) and (1b), which include information on complex formation (k_{+1i} and k_{-1i}), electron transfer (k_{+2i} and k_{-2i}) and complex dissociation (k_{+3i} and k_{-3i}), involving redox centre *i*:

$$k_{+i} = \frac{k_{+1i}\,k_{+2i}\,k_{+3i}}{k_{-1i}\,k_{-2i} + k_{-1i}\,k_{+3i} + k_{+2i}\,k_{+3i}} \quad (1a)$$

$$k_{-i} = \frac{k_{-1i}\,k_{-2i}\,k_{-3i}}{k_{-1i}\,k_{-2i} + k_{-1i}\,k_{+3i} + k_{+2i}\,k_{+3i}} \quad (1b)$$

The kinetic models presented in this article are collisional models, which are applicable to systems for which the steady-state approximation is valid and ET is rate-limiting, that is, there is fast equilibrium of the electron donor/electron acceptor complex before ET takes place.[7] Under these conditions, $k_{+i} = (k_{+1i}/k_{-1i})\,k_{+2i}$ and $k_{-i} = (k_{-3i}/k_{+3i})\,k_{-2i}$, which are products of binding constants and ET rates.

The simplest possible description of the kinetics of reduction of a multicentre redox protein is applicable when each centre reacts independently with the electron donor, in the absence of intramolecular electron exchange. In that case the protein would act as a cluster of independent monocentre proteins and the forms in which, for example, one of the centres is reduced while the rest remain oxidised are then distinct species, or states, that correspond to the same stage in the overall process of reduction. The reduction of a protein with *N* redox centres is then described by the sum of *N* exponentials with amplitudes directly related to the reduction of a particular centre. However, the assignment of each rate constant to a specific centre is possible only if the centres are spectroscopically distinguishable in the kinetic experiment. It should be noted that this simple model is of limited use because intramolecular electron exchange is usually significant, as a result of the small distances that separate redox centres inside protein molecules.[8a,b] There are, however, several multimeric proteins in which the monomers are effectively independent.

Whereas intramolecular electron exchange is usually fast, intermolecular exchange between identical protein molecules is unlikely to be physiologically significant, and it can be minimised experimentally to mimic the physiological situation. We shall, therefore, focus on the derivation of kinetic models for systems in which intramolecular electron exchange is fast and intermolecular electron exchange is slow, both on the time scale of the experiment. The immediate consequence of fast intramolecular ET is the existence of thermodynamic equilibrium between states with the same number of reduced centres that we shall refer to as the microstates of a redox stage.

For the sake of simplicity, but without loss of generality, we shall illustrate the discussion by referring to a molecule with only two redox centres and irreversible electron transfer steps, as appropriate for a strong reducing agent. The assumption of irreversibility is necessary only in order to present analytical solutions to the rate equations, but the conclusions concerning the relationship of macroscopic and microscopic rate constants are also applicable to reversible reactions. The kinetic scheme for the two-centre system, going from the oxidised to the reduced form, comprises four microsteps that interconvert the four redox microstates (Scheme 3). When intramolecular electron exchange is fast on the experimental time scale, the relative populations of

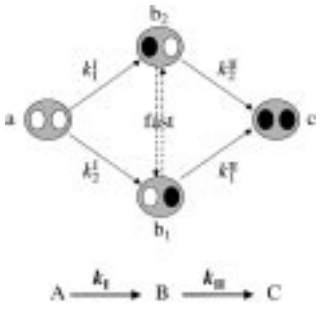

Scheme 3. *Kinetic scheme for the reduction of a two-centre protein. The pseudo-first-order rate constants for the reduction of centre* i *in the first and in the second ET steps are* k_i^I *and* k_i^{II}*, respectively. Microstates are labelled with lower case and the macroscopic stages by capital letters. Dashed arrows indicate fast equilibration between microstates* b_1 *and* b_2*, where the subscript indicates the centre which remains oxidised. The kinetic scheme for the macroscopic populations is shown in the bottom part. In this consecutive* mechanism, $\mathbf{k}_I$ *and* $\mathbf{k}_{II}$ *are the macroscopic pseudo-first-order rate constants for the first and second electron transfer steps, respectively.*

microstates (b_1 and b_2) reach thermodynamic equilibrium before the next reduction step and can be expressed as a fraction of the total population of molecules with one centre reduced (redox stage B). These fractions depend exclusively on the relative microscopic redox potentials of the two centres. Under these circumstances the complex kinetic scheme of four microscopic redox steps collapses into a simple system of two consecutive one-electron steps with macroscopic rate constants $\boldsymbol{k}_I$ and $\boldsymbol{k}_{II}$.

The relative values of $\boldsymbol{k}_I$ and $\boldsymbol{k}_{II}$ define the shape of the kinetic trace, that is, the shape of the curve of reduced fraction versus time. For a kinetic mechanism of two consecutive irreversible steps, the time dependence of the concentration of the stages A, B and C is given by Equations (2a – c):

$$[A] = [A]_0 e^{-k_I t} \quad (2a)$$

$$[B] = [A]_0\left(\frac{k_I}{k_{II} - k_I}\right)(e^{-k_I t} - e^{-k_{II} t}) + [B]_0 e^{-k_{II} t} \quad (2b)$$

$$[C] = [A]_0\left(1 - \frac{k_{II}}{k_{II} - k_I} e^{-k_I t} + \frac{k_I}{k_{II} - k_I} e^{-k_{II} t}\right) + [B]_0(1 - e^{-k_{II} t}) + [C]_0 \quad (2c)$$

where $[A]_0$, $[B]_0$ and $[C]_0$ are the concentrations of the stages at time zero, such that $[B]_0 = [C]_0 = 0$ in a fully oxidised sample. Since one centre is reduced in stage B and two centres are reduced in stage C, the global reduced fraction for a sample which is fully oxidised at time zero is given by Equation (3):

$$\frac{[B] + 2[C]}{2([A] + [B] + [C])} = 1 + \frac{k_I - 2k_{II}}{2(k_{II} - k_I)} e^{-k_I t} + \frac{k_I}{2(k_{II} - k_I)} e^{-k_{II} t} \quad (3)$$

Note that the result for the global reduced fraction is the sum of two exponentials with variable amplitudes that may even be negative, and that the rate constants are not simply those of the two individual centres.

If $\boldsymbol{k}_I \gg \boldsymbol{k}_{II}$, the curve is biphasic with equal amplitudes and the two rate constants are readily accessible from the data (Figure 1a). This situation is typical since $\boldsymbol{k}_I$ will be twice as large as $\boldsymbol{k}_{II}$ if all of the microscopic rate constants are equal, simply because both centres are available to accept electrons in the first step. When $\boldsymbol{k}_I \approx \boldsymbol{k}_{II}$, the observed kinetic trace is approximately monophasic (Figure 1b). The expressions in Equations (2b) and (2c) are undefined when $\boldsymbol{k}_I = \boldsymbol{k}_{II}$ exactly; integration of the rate equations then gives Equation (4):

$$[B] = \{\boldsymbol{k}t[A]_0 + [B]_0\} e^{-kt} \quad (4)$$

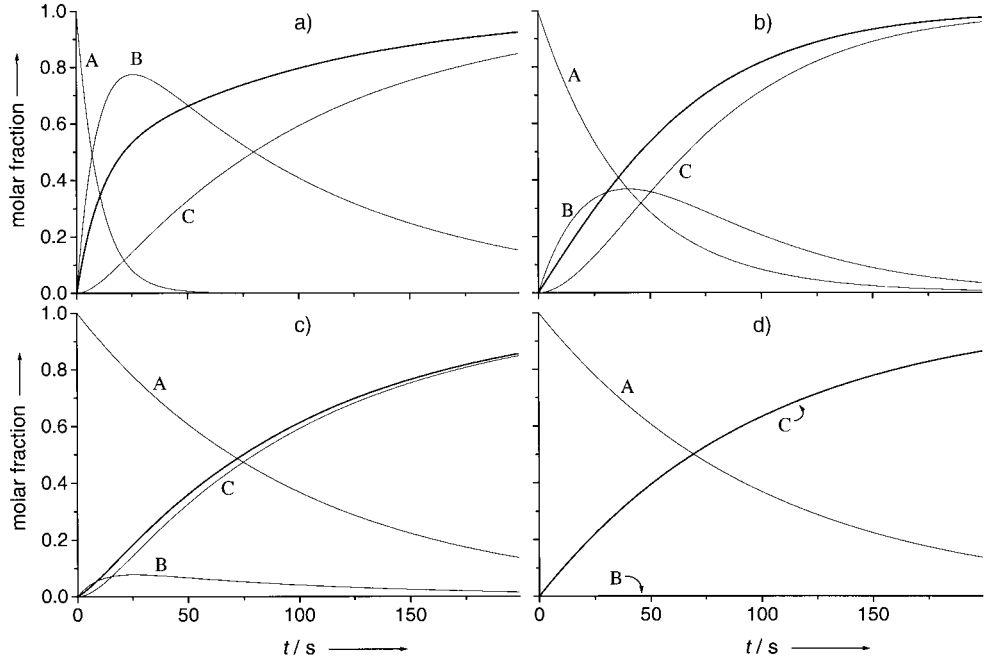

Figure 1. *Simulated kinetic traces for the reduction of a fully oxidised two-centre system with a variety of macroscopic pseudo-first-order rate constants. The global reduced fraction is shown as a thick line and the populations of the individual redox stages are shown as fine lines. Equations (2a – c), (3) and (4) were used to generate the curves. a)* $\mathbf{k}_I = 10^{-1}\,s^{-1}$, $\mathbf{k}_{II} = 10^{-2}\,s^{-1}$; *b)* $\mathbf{k}_I = \mathbf{k}_{II} = 2.5 \times 10^{-2}\,s^{-1}$; *c)* $\mathbf{k}_I = 10^{-2}\,s^{-1}$, $\mathbf{k}_{II} = 10^{-1}\,s^{-1}$; *d)* $\mathbf{k}_I = 10^{-2}\,s^{-1}$, $\mathbf{k}_{II} = 10^{2}\,s^{-1}$.

in place of Equation (2b), and the result for [C] follows from the conserved total protein concentration. When $k_I < k_{II}$ there may be an apparent lag phase because one of the exponential components has a negative amplitude (Figure 1c). The limiting case for $k_I \ll k_{II}$ is purely monophasic and only the rate constant of the slower step can be determined from an experiment starting from the fully oxidised state (Figure 1d).

It remains possible to determine the faster rate constant when $k_I < k_{II}$ by making use of experiments starting from thermodynamic equilibrium in partially reduced samples. Then there will be some fraction of molecules in state B available for reduction to state C with the fast rate constant, resulting in a biphasic curve from which both k_{II} and k_I can be determined. In the case of redox centres displaying very different reduction potentials, virtually all molecules in a 50% reduced sample at thermodynamic equilibrium are in state B (Figure 2a). This is quite different

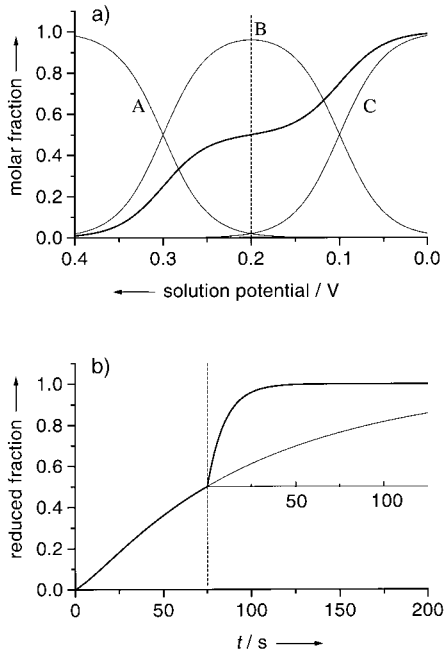

Figure 2. *The global reduced fraction (thick lines) and the populations of stages at thermodynamic equilibrium as a function of solution potential and the reduced fraction during a kinetic experiment as a function of time. a) Simulation of the populations at equilibrium for a two-centre protein with noninteracting midpoint potentials* $e_1 = 0.3$ *V,* $e_2 = 0.1$ *V and* $I_{12} = 0$ *V. b) Time evolution of the reduced fraction for the kinetic trace represented in Figure 1c,* $k_I = 10^{-2}\,s^{-1}$, $k_{II} = 10^{-1}\,s^{-1}$. *The inset curve shows the result for starting from a 50% reduced sample at thermodynamic equilibrium. Note that this behaviour is compatible with model 2 (discussed in the following section), but not with model 1.*

from the population of state B at 50% reduction in the kinetic experiment presented, for example, in Figure 1c. In this case, with $k_I < k_{II}$, an approximately monophasic trace with the slower rate constant is observed in an experiment starting from the oxidised form, and another monophasic trace with the faster rate constant is observed in an experiment starting from a 50% reduced sample (Figure 2b). In fact, if the kinetic run could be interrupted at 50% reduction and the sample given time to reach thermodynamic equilibrium before restarting, then the trace would follow the thick line in Figure 2b.

Although the rate constants of the macroscopic steps, k_I and k_{II} in the two-centre system, are accessible from the experimental data, they do not give direct information about the kinetic properties of the individual redox centres. Equations (5a) and (5b) relate these macroscopic rate constants and the rate constants of the microsteps (see Scheme 3):

$$k_I = k_1^I + k_2^I \quad (5a)$$

$$k_{II} = \chi_1 k_1^{II} + \chi_2 k_2^{II} \quad (5b)$$

where k_i^I and k_i^{II} are the rate constants for the reduction of centre i in steps I and II, respectively, and χ_i is the molar fraction of the microstate which has centre i oxidised in stage B and, consequently, still available to receive an electron. These equations show that the macroscopic rate constant of each step is given by the weighted average of the microscopic rate constants of all microsteps involved in that particular step. As will be discussed below, the rate constants of the individual centres can change between step I and step II for a variety of reasons, including a change of the driving force for the electron transfer process due to interactions between the redox centres. The key question is whether it is possible to define them unequivocally from the experimentally accessible macroscopic rate constants for each step, k_s.

The problem of deriving microscopic constants from macroscopic properties is commonly associated with the possibility of distinguishing the redox centres spectroscopically in the kinetic experiment. However, the existence of different spectroscopic characteristics is not important under conditions of fast intramolecular electron transfer. In fact, the order of reduction of the centres that is observed in a kinetic experiment under these conditions is dictated by the thermodynamics of the system. This is easily demonstrated by considering two centres with very different redox potentials ($e_1 \gg e_2$) which display different spectroscopic characteristics. If the rate constant for the reduction of centre 1 is larger than the rate constant for the reduction of centre 2 ($k_1^I > k_2^I$), then the kinetic experiments will show centre 1 being reduced at a higher rate than centre 2, as expected. However, even if $k_1^I < k_2^I$, centre 1 will still become reduced before centre 2 because of intramolecular electron transfer. Centre 2 is actually being reduced by the exogenous electron donor at a faster rate than centre 1, but the electrons are immediately transferred, or "drained", to centre 1, according to the relative redox potentials. Consequently, the observed order of reduction of the redox centres under conditions of fast intramolecular ET will always reflect their relative redox potentials, that is, their thermodynamic properties, and not necessarily their relative kinetic properties. It is clear from this example that the problems associated with the determination of the rate constants of the individual centres are not related to the possibility of monitoring the redox centres separately but do depend on knowing the microscopic thermodynamic properties of the centres.

Application of the Marcus theory

Because only N rate constants can be obtained from the experimental data for a system with N centres and fast intramolecular ET ($\boldsymbol{k}_{\mathrm{I}}$ and $\boldsymbol{k}_{\mathrm{II}}$ in the two-centre system, in which there are four microscopic rate constants), it is necessary to reduce the number of unknowns by making approximations. Two possible approaches will be discussed below in which it is assumed that the ET step is rate-determining.[7] It will be shown that the determination of the rate constants of the microsteps depends upon the accurate determination of the thermodynamic properties of the individual redox centres.

The Marcus equation for ET rates[2] may be applied with the simplification that electrostatic interactions can be neglected in solutions of moderate ionic strength, and also neglecting orientation effects, which is particularly suitable for small reducing agents. Each microscopic rate constant of the kinetic scheme (Scheme 3) may then be expressed [Eq. (6)] as a function of a factor, Z, with the dimensions of a collision frequency, the reorganisation energy, λ, and the driving force for the ET reaction, ΔG:

$$k = Z\exp[-(\Delta G+\lambda)^2/(4\lambda RT)] \quad (6)$$

The effect of the binding constant, distance between redox centres, and the intervening medium are included in the factor Z. The value of ΔG may be calculated for any individual microstep because it depends solely on the thermodynamic parameters of the system, which may be accessible from equilibrium experiments. It may vary between microsteps because of intrinsic differences in the microscopic reduction potentials of the centres and also because the potential of each individual centre may change with the overall stage of reduction. Therefore, it is useful to rewrite Equations (5a) and (5b) to separate the effect of ΔG from the effect of Z and λ and also to separate the variable microscopic reduction potentials of the centres, e_i, from the reduction potential of the donor, e_{D}. We define a reference rate constant for each microstep in which the microscopic reduction potential of the centre is set equal to zero. Thus, for example, k_i^{os} is the reference rate constant for the reduction of centre i in step s. Now the actual rate constants of the microsteps, $k_i^{s\tau}$, are related to the reference rates by factors $\gamma_i^{s\tau}$, defined by Equation (7).

$$\gamma_i^{s\tau} = \exp\left[\frac{\mathrm{e}_i^{s\tau}F}{2RT}\left(1+\frac{\mathrm{e}_{\mathrm{D}}F}{\lambda_i^{s\tau}}-\frac{\mathrm{e}_i^{s\tau}F}{2\lambda_i^{s\tau}}\right)\right] \quad (7)$$

The labelling of each rate constant must specify the macroscopic redox step, s, the centre involved, i, and the state of all the other centres in the system that remain unchanged in the microstep, τ. We shall use these labels in the form $k_i^{s\tau}$, but the specification τ is not necessary in a system with just two centres because there is only one microstep per centre in each macroscopic step. Therefore, Equations (5a) and (5b) may be rewritten in the form of Equations (8a) and (8b):

$$\boldsymbol{k}_{\mathrm{I}} = \gamma_1^{\mathrm{I}}k_1^{o\mathrm{I}}+\gamma_2^{\mathrm{I}}k_2^{o\mathrm{I}} \quad (8a)$$

$$\boldsymbol{k}_{\mathrm{II}} = \chi_1\gamma_1^{\mathrm{II}}k_1^{o\mathrm{II}}+\chi_2\gamma_2^{\mathrm{II}}k_2^{o\mathrm{II}} \quad (8b)$$

where χ_i and γ_i^s depend solely on the thermodynamic parameters of the system, $k_i^{o\mathrm{I}}$ are the microscopic rate constants for the reference in the first reduction step, and $k_i^{o\mathrm{II}}$ are the corresponding rate constants for the second reduction step.

Differences between the microscopic reduction potentials of the centres are intrinsic, but interactions between centres provide the key to many functional properties. Therefore, it may be useful to divide the factors of Equation (7) into terms that depend on the redox potentials of the centres in some reference state and terms that depend on changes in the driving force. We shall consider a microstep that involves centre i in step s while the remaining centres remain unchanged in a state that we label collectively as τ. Step $s+1$ contains microsteps that involve centre i and the remaining centres in a state τ' that differs from τ simply by a change of state of one centre, j. A factor is then defined as $\sigma_{ij}^s=\gamma_i^{s\tau}/\gamma_i^{(s+1)\tau'}$. For example, there is only one sigma factor for each centre in the case of a two-centre system, $\sigma_{ij}=\gamma_i^{\mathrm{I}}/\gamma_i^{\mathrm{II}}$. If the reorganisation energy, λ_i, does not change from step to step, the sigma factor is a simple function [Eq. (9)] of the change in the driving force between steps, δG_{ij}:

$$\sigma_{ij}^s = \exp\left[\frac{-\delta G_{ij}}{2RT}\left(1+\frac{\Delta G_i^{(s+1)\tau'}}{\lambda_{\mathrm{i}}}+\frac{\delta G_{ij}}{2\lambda_{\mathrm{i}}}\right)\right] \quad (9)$$

where $\delta G_{ij}=\Delta G_i^{s\tau}-\Delta G_i^{(s+1)\tau'}$ if the convention of referring energies to those of the reduced form is used.[9] The driving force used as a reference in this article is ΔG_i for the last reduction step, that is, ΔG_i^N for a system with N centres, which is equal to $(e_{\mathrm{D}}-e_i^N)F$. The change in the driving force between the last step and the penultimate step depends on the interaction potential between the centres, $\delta G_{ij}=-I_{ij}\mathrm{F}$, and so on. Now a single gamma factor can be defined for each centre [Eq. (10)] and the superscript $s\tau$ used to specify individual microsteps can be dropped:

$$\gamma_i = \exp\left[\frac{e_i^NF}{2RT}\left(1+\frac{\mathrm{e}_{\mathrm{D}}F}{\lambda_{\mathrm{i}}}-\frac{e_i^NF}{2\lambda_{\mathrm{i}}}\right)\right] \quad (10)$$

The reorganisation energy, λ_i, associated with each centre is difficult to determine, but it may not be crucial to have an exact value since the reference potential for the centre, e_i^NF, and the potential for the donor, $e_{\mathrm{D}}F$, are usually much smaller than λ_i. The gamma factor of Equation (10) can then be approximated by Equation (11), in which the γ_i factors depend exclusively on the

$$\gamma_i \approx \exp\left(\frac{e_i^NF}{2RT}\right) \quad (11)$$

reduction potential of centre i in the reference state. Similarly, the driving force, ΔG_i, for ET reactions in biological systems and the interaction energies, $I_{ij}F$, are typically much smaller than the reorganisation energy λ_i.[10] Thus, Equation (9) can be approximated by Equation (12), in which σ_{ij} depends solely on the

$$\sigma_{ij} \approx \exp\left(\frac{I_{ij}F}{2RT}\right) \quad (12)$$

interaction potential between the two redox centres. In other words, σ_{ij} is a function of the change of the driving force along the reduction process only. Moreover, because microscopic

reversibility implies that $I_{ij} = I_{ji}$, only one sigma factor is required for a two-centre system under this approximation. Even so, it is preferable to obtain a reasonable value for the reorganisation energy and use the full expression.

A factor similar to that in Equation (12) was used in an earlier study of a tetrahaem cytochrome c_3, without reference to the Marcus theory.[11] In effect, the multiplier of *RT* was treated as a variable, but the value 2 was preferred on the grounds of treating oxidation and reduction symmetrically. Here, the factor emerges directly from the theory as a result of the assumptions that $\lambda_i \gg \Delta G_i$ and $\lambda_i \gg I_{ij}$F. The factor in Equation (11) refers to the microscopic potentials in a single reference state (e.g. stage *N*, the fully reduced protein), and the relative rates of microsteps in successive steps can be obtained by multiplying $\gamma_i k_i^o$ by one sigma factor for each step.

Equations (8a) and (8b) can now be written in the form of Equations (13a) and (13b).

$$\boldsymbol{k}_{\mathrm{I}} = \gamma_1 \sigma_{12} k_1^{\mathrm{oI}} + \gamma_2 \sigma_{21} k_2^{\mathrm{oI}} \quad (13\,\mathrm{a})$$

$$\boldsymbol{k}_{\mathrm{II}} = \chi_1 \gamma_1 k_1^{\mathrm{oII}} + \chi_2 \gamma_2 k_2^{\mathrm{oII}} \quad (13\,\mathrm{b})$$

At this point, the difference in the microscopic redox potentials of the centres of the reduced protein have been separated in the form of gamma factors, and the variation in potentials due to interactions is accounted for by the sigma factors. However, since there are still four reference rate constants for the microscopic steps and only two observables, further assumptions are needed to reduce the number of unknowns.

First, we shall consider proteins with redox centres in very different environments and very different exposure to the solvent, for which it might be reasonable to assume different *Z* factors and reorganisation energies for each centre. However, it is then necessary to assume that these values are fixed and do not change from one step to the next. Thus, the rate constants are assumed to be modulated by ΔG_i only, and there is only one reference rate that can be adjusted for each centre, that is, $k_i^{\mathrm{oI}} = k_i^{\mathrm{oII}} = k_i^o$ in the two-centre system, with k_1^o and k_2^o as variables [Eqs. (14a) and (14b)].

$$\boldsymbol{k}_{\mathrm{I}} = \gamma_1 \sigma_{12} k_1^o + \gamma_2 \sigma_{21} k_2^o \quad (14\,\mathrm{a})$$

$$\boldsymbol{k}_{\mathrm{II}} = \chi_1 \gamma_1 k_1^o + \chi_2 \gamma_2 k_2^o \quad (14\,\mathrm{b})$$

We shall refer to this set of assumptions as model 1. The number of unknowns is equal to the number of observables, but the model can only fit experimental data if the rates are under thermodynamic control *and* the *Z* factors and reorganisation energies of each centre are not dependent on the global oxidation state of the protein.

The second approach, model 2, is suitable for proteins in which the centres have similar environments and similar exposure to the solvent but undergo significant changes in each redox step. In this case, we assume that the centres have *Z* factors and reorganisation energies that are all identical within each macroscopic redox step, but they are allowed to change from step to step, that is, they may depend on the number of electrons in the molecule. In the two-centre system, the independent variables of this model are a reference rate constant for step I, $k^{\mathrm{oI}} = k_1^{\mathrm{oI}} = k_2^{\mathrm{oI}}$, and a reference rate constant for step II, k^{oII}, that is also the same for both centres. According to this parameterisation of the system, and by using the approximations in Equations (11) and (12), Equations (8a) and (8b) can be expressed in the form of Equations (15a) and (15b):

$$\boldsymbol{k}_{\mathrm{I}} = (\gamma_1 \sigma_{12} + \gamma_2 \sigma_{21}) k^{\mathrm{oI}} \quad (15\,\mathrm{a})$$

$$\boldsymbol{k}_{\mathrm{II}} = (\chi_1 \gamma_1 + \chi_2 \gamma_2) k^{\mathrm{oII}} \quad (15\,\mathrm{b})$$

In this case, the difference between k^{oI} and k^{oII} reflects the difference in *Z* factors or reorganisation energies between the first and the second ET steps. Note that Equations (8a) and (8b) are exact, but factorisation of the thermodynamic terms depends on the approximation of the reorganisation energy being large because λ may be different for the same centre in different steps. Any system that fulfils the requirements of rapid internal equilibration, such that *N* macroscopic rate constants are observed for *N* centres, should be fitted exactly by this model. In effect, this model fits the *N* rate constants and determines the rates for the individual microsteps within a macroscopic step according to the relative driving forces, which are fixed. Thus, any discussion of the rates of individual microsteps derived from model 2 must depend on arguments that justify the specific assumptions made in the model and not simply on the ability to fit the data.

The approximations made in each of the models achieve the aim of reducing the number of variables that link the rate constants of the macroscopic electron transfer steps to those of the individual redox centres to equal *N*, the number of observables. However, the factors require detailed information about the thermodynamic properties of the system.

For ET reactions between protein complexes that are physiological partners, specific protein – protein interactions make ET most likely to occur through a single binding, or docking, site. This would apply to membrane-bound proteins with little surface exposure. In this case, the rate constants for electron transfer for each centre are essentially controlled by the distance to the docking site. Since only model 1 allows the values of k_i^o to be adjusted independently of the relative value of ΔG_i for the ET process, it is, in principle, more appropriate than model 2 for describing ET reactions between physiological partners. In the example of a two-centre protein, if the centres are associated with sites that display significantly different binding constants for the electron donor, then the characteristics of the kinetic trace will tell immediately if the strongest interaction is in the vicinity of the centre with the largest driving force. If the centre with smaller driving force is associated with the docking site, then the kinetic trace will be approximately monophasic (see Figure 1b). This is because the faster intramolecular electron exchange will keep the "entry gate" centre free to receive electrons from the external donor, while the other centre is being reduced by intramolecular ET. If the docking site involves the centre with the larger driving force, the kinetic trace will be

biphasic (Figure 1 a), with the biphasic character increasing with the separation between the reduction potentials of the centres.

Generalisation to systems with more than two redox centres is straightforward and is subject to the same limitations. To extract kinetic information for individual centres, it is necessary that: 1) the thermodynamic properties are characterised in detail, and 2) some model is used to relate individual rates. Application of the Marcus theory allows the number of variables to be reduced either by assuming that Z and λ are equal for all centres within a given ET step or that Z and λ are different for each centre, but do not change as the protein is reduced.

Analysis of the kinetics of reduction of a tetrahaem protein

We shall now illustrate the application of the theory to the reduction of *Desulfovibrio gigas* tetrahaem cytochrome c_3 by sodium dithionite. The thermodynamic properties of this protein have been thoroughly investigated[3, 12, 13] and NMR spectroscopic studies have shown that intramolecular ET is fast on the time scale of stopped-flow experiments.[12] However, intermolecular ET between cytochrome c_3 molecules can be neglected because it is at least 100 times slower than ET from sodium dithionite.[11, 12]

The effective midpoint redox potential of sodium dithionite (ca. -0.5 V) is sufficiently negative[4] to ensure that ET proceeds from the exogenous donor to the cytochrome only, leading to irreversible ET steps. Moreover, the use of a large excess of sodium dithionite makes the process pseudo-first order. Because the concentration dependence of the rates shows that the SO_2^- radical is the reducing species,[5, 11] the relevant value of e_D is that of the SO_2^-/SO_2 couple. Thermodynamic calculations[14] and direct experiments[6] provide a value of -0.3 V at 298 K that is pH-independent above pH 2.

Early NMR studies showed that the midpoint redox potentials of the four haems depend on the redox state of the neighbouring haems and also on the pH.[12] In a study by Coletta et al.,[13] the protein was treated as having fundamentally different properties in its acidic and basic forms, with 21 thermodynamic parameters. Fitting these by grid searching in 10-mV steps obscured the fact that they are not well defined. In fact, 15 parameters are sufficient to describe the system in the framework of a model with five interacting centres since only two-centre interactions are required.[9] Thus, there is no evidence for major proton-linked changes in conformation. These microscopic parameters, namely the four midpoint potentials of the haems and the pK_a of the acid/base group in the reference state, plus six haem–haem interaction potentials and four haem–proton interaction potentials have all been determined for *D. gigas* cytochrome c_3.[3] The complete description of the system involves 16 protonated and 16 deprotonated microstates, which are in equilibrium because proton exchange is fast. Upon reaction with the electron donor these 32 microstates are interconverted through 64 possible ET microsteps. Therefore, the complete kinetic characterisation of this protein at the microscopic level involves the determination of 64 microscopic rate constants (Figure 3). As discussed above, the existence of

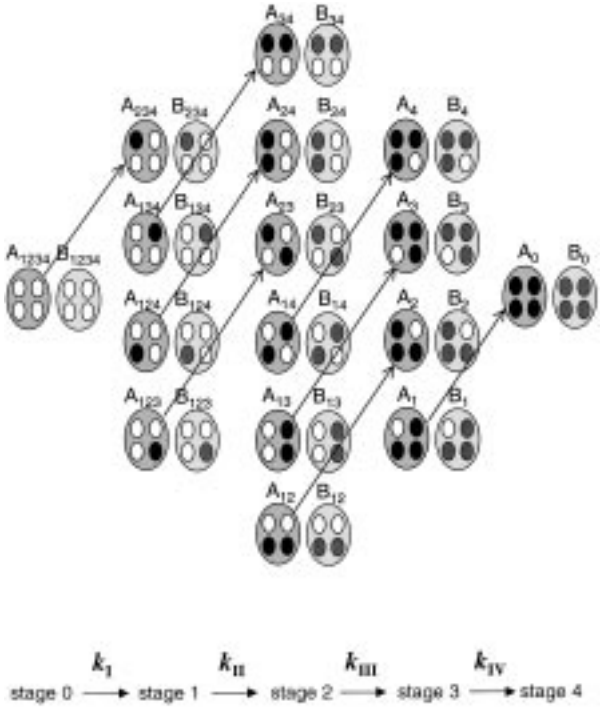

Figure 3. *Schematic representation of the microstates of a protein with four redox centres and one acid/base centre. For simplicity only the eight ET microsteps involving one centre in the protonated form are indicated out of a total of 64. Protonated microstates are represented by A and deprotonated microstates by B, subscripts indicate the centres that are oxidised in each microstate. Because of fast intramolecular electron and proton transfer between microstates that belong to the same redox stage, the complex kinetic scheme collapses into the simple mechanism of four consecutive one-electron transfer steps with only four macroscopic rate constants, shown in the bottom part of the figure. Redox stages are defined according to the number of reduced centres and* $\mathbf{k}_I - \mathbf{k}_{IV}$ *are the macroscopic pseudo-first-order rate constants for the four consecutive one-electron transfer steps. Note that a system with* N *centres gives rise to* $N+1$ *different redox stages (numbered* $n = 0,\ldots N$*), each of which comprises* C_n^N microstates, where C *is a binomial coefficient. These stages are linked by* N *macroscopic redox steps (numbered* $s = 1,\ldots N$*), each of which comprises* sC_s^N microscopic redox steps. Within step s, *each of the* N *centres is involved in* C_{s-1}^{N-1} of the microsteps.

fast equilibrium within microstates belonging to the same stage leads to a much simpler kinetic scheme of four consecutive one-electron steps. Consequently, a maximum of four rate constants are available from experimental data and, in practice, the kinetic traces appear to be no more than biphasic. Thus, unless further assumptions are used to limit the number of variables to a maximum of four, the system is undefined.

Two different approaches to this problem have been described here: In model 1 the four haems have different Z factors and reorganisation energies and these parameters remain unchanged throughout the reduction process; in model 2 the four haems have identical Z factors and reorganisation energies, but these parameters may depend on the number of electrons in the molecule and change from step to step. In both cases the effect of ΔG on the rate constants is accounted for by introducing the appropriate gamma and sigma factors. Generalisation of Equations (14 a) and (14 b) for applying model 1 to the tetrahaem cytochrome is straightforward [Eqs. (16 a–d)] if it is

assumed that the Z factor and reorganisation energy for each centre is unaffected by protonation:

$$\boldsymbol{k}_{\mathrm{I}} = \sum_i \gamma_i \sigma_{ij}\sigma_{ik}\sigma_{il}(\chi^{\mathrm{A}}_{ijkl} + \sigma_{i\mathrm{H}}\chi^{\mathrm{B}}_{ijkl})k^{\circ}_i \quad (16\,\mathrm{a})$$

$$\boldsymbol{k}_{\mathrm{II}} = \sum_i \gamma_i \left(\sum_{jk} \sigma_{ij}\sigma_{ik}\chi^{\mathrm{A}}_{ijk} + \sigma_{i\mathrm{H}}\sum_{jk}\sigma_{ij}\sigma_{ik}\chi^{\mathrm{B}}_{ijk}\right)k^{\circ}_i \quad (16\,\mathrm{b})$$

$$\boldsymbol{k}_{\mathrm{III}} = \sum_i \gamma_i \left(\sum_{j} \sigma_{ij}\chi^{\mathrm{A}}_{ij} + \sigma_{i\mathrm{H}}\sum_{j}\sigma_{ij}\chi^{\mathrm{B}}_{ij}\right)k^{\circ}_i \quad (16\,\mathrm{c})$$

$$\boldsymbol{k}_{\mathrm{IV}} = \sum_i \gamma_i(\chi^{\mathrm{A}}_i + \sigma_{i\mathrm{H}}\chi^{\mathrm{B}}_i)k^{\circ}_i \quad (16\,\mathrm{d})$$

The macroscopic rate constants, $\boldsymbol{k}_{\mathrm{I}}$, $\boldsymbol{k}_{\mathrm{II}}$, $\boldsymbol{k}_{\mathrm{III}}$ and $\boldsymbol{k}_{\mathrm{IV}}$, are simply the weighted average of all microscopic rate constants that contribute to each particular step. The weighting factors are the relevant fractional populations, χ_{ijkl}, χ_{ijk}, χ_{ij}, χ_i, where subscripts indicate the haems which are oxidised and superscripts A and B refer to protonated and deprotonated microstates, respectively (Figure 3). The midpoint potentials of the haems contribute to the microscopic rate constants through the gamma factors γ_i, defined in Equation (10), which refer to the driving force for each centre in the final step to the fully reduced state of the protonated protein. The factors σ_{ij} account for haem–haem interaction potentials, I_{ij}, according to Equation (9). The $\sigma_{i\mathrm{H}}$ factors are exactly analogous to the factors in Equation (9) for interactions between redox centres and account for haem–proton interaction potentials, $I_{i\mathrm{H}}$. Because haem–haem interaction potentials have been defined between the haem that is being reduced and those haems that remain oxidised, products of three σ_{ij} factors contribute to the rate constants of the first reduction step, products of two σ_{ij} factors contribute to the rate constants of the second reduction step, and so on. No σ_{ij} factors are necessary in the last reduction step, which provides the reference rates for each centre. According to this model, the four parameters to be adjusted are the rate constants of four hypothetical haems with zero midpoint potential, k°_i. These constants account for the difference in Z factors and reorganisation energies between the four haems.

If model 2 is used, the approximations of Equations (11) and (12) allow expressions of exactly the same form as Equations (16a–d), but with the reference rates for each centre, k°_i, replaced by the reference rates of the macroscopic steps, k^{os}. As before, the gamma factors defined in Equation (7) for individual microsteps, labelled $s\tau$, can be used to provide exact expressions if the values of λ are known. The four parameters to be adjusted are now k^{oI}, k^{oII}, k^{oIII} and k^{oIV}, which correspond to the rate constants of a hypothetical haem with zero midpoint potential in each particular step.

The kinetics of reduction of cytochrome c_3 from *Desulfovibrio gigas* by sodium dithionite display a biphasic profile with a fast phase accounting for ca. 25% of the process.[11] An experiment starting from partially reduced samples showed that the fast phase disappears if the sample at time zero is more than 30% reduced. The fast phase also disappears at low pH because the rate of the slower phase increases. In this cytochrome, haem 4 is almost fully reduced in step 1, whereas the other haems are still mostly oxidised. The remaining haems all have similar, more negative, midpoint redox potentials, which makes it difficult to separate them kinetically. According to model 1, the rapid reduction of haem 4 could arise either through rapid reaction of haem 4 itself or through reduction of another centre followed by intramolecular ET. However, if electrons were being drained to haem 4 rather than delivered directly, the fast phase should account for more than 25% of the process. Thus the shape of the complete curve should be capable of distinguishing the possibilities. From the point of view of model 2, the initial 25% fast phase clearly corresponds to a larger rate constant for the first step, k^{oI}, regardless of whether haem 4 is reduced directly or indirectly, and the 75% slow phase corresponds to slower rate constants for the subsequent steps, k^{oII}, k^{oIII} and k^{oIV}.

The test of the analysis is to fit kinetic traces obtained at different pH values and with varying degrees of reduction in the starting material. Kinetic experiments were carried out in a SF-61 Hi-Tech Scientific stopped-flow apparatus inside an anaerobic chamber. Absorbance changes were monitored at 552 nm. Concentrations after mixing were [cytochrome c_3] = 1.5 μM, [dithionite] = 65 μM, and 50 mM tris/maleate buffer. The temperature was maintained at 25 °C. The theory discussed above predicts that each trace yields a maximum of four macroscopic rate constants and that the complete set of data can be fitted with a maximum of four variables, with the set of predetermined thermodynamic parameters taken from ref. [3].

Using the Marquardt method to fit a set of traces, with a value of 1 eV for the reorganisation energy[15] and independent parameters for the four haems (model 1), gave rates close to zero for haems 2 and 3. Therefore, these rates were fixed at zero and the resulting simulations, shown in Figure 4, have only two

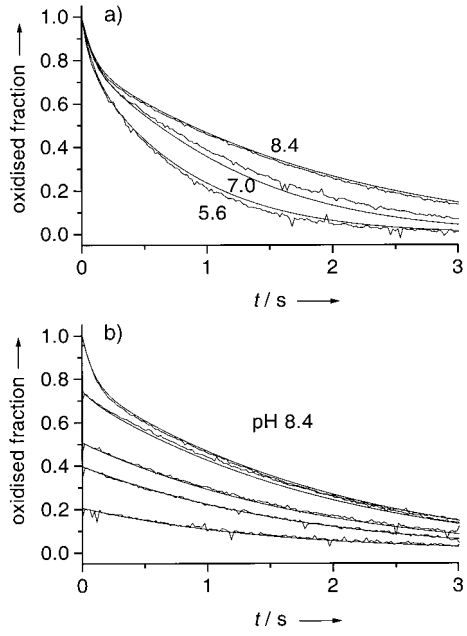

Figure 4. *Kinetics of reduction of cytochrome* c_3 *from* Desulfovibrio gigas *by sodium dithionite. Solid lines were obtained by fitting all of the data simultaneously to model 1 using only two parameters:* $k^{\circ}_i = (7.7 \pm 0.5) \times 10^8\,\mathrm{M^{-1}s^{-1}}$, $k^{\circ}_4 = (5.8 \pm 0.9) \times 10^8\,\mathrm{M^{-1}s^{-1}}$. *The rate constants for haems 2 and 3 were set to zero. a) Reduction of oxidised samples at pH 5.6, 7.0 and 8.4; b) reduction of partially reduced samples at pH 8.4.*

fitted parameters. Fitting the traces according to model 2, with independent rates for the four ET steps, gave fits of similar quality.

Figure 4 shows that the full range of behaviour, both as a function of pH and of the degree of reduction of the initial samples, is well described by model 1 with a set of predetermined thermodynamic parameters[3] and just two fitted rate constants. This is in contrast with earlier analyses of similar data in which as many as eight parameters were used,[11] following the thermodynamic analysis in terms of fundamentally different acidic and basic forms.[13] However, it appears that the kinetic properties are adequately described by treating the protonation as just one more factor that affects the driving force, through the redox-Bohr interactions with the proton, without changing the reorganisation energy significantly with respect to the corresponding microstep in the protonated form. The same conclusion follows from the ability to fit the pH dependence of the kinetic traces using model 2.

The two models also agree that haem 4 is the primary electron acceptor in step I. According to model 2, the majority of the flux of electrons in step I passes through haem 4 because it has the largest driving force. In model 1, although the reference rate fitted for haem 1 is larger than that for haem 4, the actual rate for the microstep involving haem 4 in step I is much greater than that of haem 1, again as a result of its larger driving force. In the case of the reduction of cytochrome c_3 by sodium dithionite, model 1 is arguably more appropriate because, although each of the four haems is exposed to the reducing agent, the local charges and collision frequencies are likely to be different. As discussed above, model 1 is more restrictive, and yet it fits the data as well as model 2. However, the molecule also undergoes subtle conformational changes upon reduction,[16] which would favour the assumptions made in model 2. Thus, in this particular case, conclusions about the kinetic properties of the individual centres will be most reliable when the results of the two models agree.

In practice, model 1 and model 2 represent simplifications that are necessary to extract information about the many microscopic redox steps, and hence the individual centres, from the few observable macroscopic rate constants. The true situation in most cases is likely to be a mixture of the two. The fact that the kinetics of reduction of cytochrome c_3 by sodium dithionite can be described simply in terms of the thermodynamic interactions between the redox centres and with an acid/base group does not rule out the possibility that the rate constants may also be influenced by, for example, variations in the charge on the surface of the protein, but the observable properties provide no further information.

Conclusion

The models discussed here, with the appropriate approximations, appear to be fully adequate for the analysis of the kinetic properties of systems under thermodynamic control, in which case a protein with *N* redox centres yields a kinetic trace with a maximum of *N* exponential components. Therefore, the limitations of the information that may be extracted are clear, both in terms of the number of parameters and their physical significance. Model 2 fits the time constants with reference rates for these macroscopic steps and apportions the rates for individual microsteps according to the relative driving force. Thus, the quality of fit should provide a test of the experimental data as well as the assumption of thermodynamic control. However, model 2 implies that the centres have equal accessibility as well as equal reorganisation energies, which may be unrealistic. Model 1 is more restrictive, insofar as any change in rate from one macroscopic step to the next can only be the result of the change in driving force for each of the centres, but it is more realistic for proteins with centres in widely different environments. Thus, the significance of rates obtained for individual centres or microsteps must be judged with respect to the assumptions of the model being used, and comparison of the parameters obtained with the two models should provide additional insight into their reliability.

The authors would like to thank Prof. António V. Xavier for initiating the project on kinetics of multicentre proteins and aiding the development and clarification of the models through numerous discussions. We thank Ricardo O. Louro for discussions concerning the organisation of the manuscript and Catarina Paquete for running the kinetic experiments on cytochrome c_3. *This work was supported by the EC Network (contract ERBFMRX-CT98-0218).*

[1] R. E. Sharp, S. K. Chapman, *Biochim. Biophys. Acta* **1999**, *1432*, 143 – 158.
[2] R. A. Marcus, N. Sutin, *Biochim. Biophys. Acta* **1985**, *811*, 265 – 322.
[3] R. O. Louro, T. Catarino, D. L. Turner, M. A. Piçarra-Pereira, I. Pacheco, J. LeGall, A. V. Xavier, *Biochemistry* **1998**, *37*, 15 808 – 15 815.
[4] S. G. Mayhew, *Eur. J. Biochem.* **1978**, *85*, 535 – 547.
[5] D. O. Lambeth, G. Palmer, *J. Biol. Chem.* **1973**, *248*, 6095 – 6103.
[6] P. Neta, R. E. Huie, A. Harriman, *J. Phys. Chem.* **1987**, *91*, 1606 – 1611.
[7] V. L. Davidson, *Biochemistry* **1996**, *35*, 14 035 – 14 039.
[8] a) C. C. Moser, J. M. Keske, K. Warncke, R. S. Faird, P. L. Dutton, *Nature* **1992**, *355*, 796 – 802; b) C. C. Page, C. C. Moser, X. Chen, P. L. Dutton, *Nature* **1999**, *402*, 47 – 52.
[9] D. L. Turner, C. A. Salgueiro, T. Catarino, J. LeGall, A. V. Xavier, *Eur. J. Biochem.* **1996**, *241*, 723 – 731.
[10] "Biological electron transfer chains: genetics, composition and mode of operation": P. L. Dutton, X. Chen, C. C. Page, S. Huang, T. Ohnishi, C. C. Moser, *NATO ASI Ser. Ser. C* **1998**, *512*, 3 – 8.
[11] T. Catarino, M. Coletta, J. LeGall, A. V. Xavier, *Eur. J. Biochem.* **1991**, *202*, 1107 – 1113.
[12] H. Santos, J. J. G. Moura, I. Moura, J. LeGall, A. V. Xavier, *Eur. J. Biochem.* **1984**, *141*, 283 – 296.
[13] M. Coletta, T. Catarino, J. LeGall, A. V. Xavier, *Eur. J. Biochem.* **1991**, *202*, 1101 – 1106.
[14] D. M. Stanbury, L. A. Lednicky, *J. Am. Chem. Soc.* **1984**, *106*, 2847 – 2853.
[15] H. E. M. Christensen, I. Coutinho, L. S. Conrad, J. M. Hammerstad-Pedersen, G. Iversen, M. H. Jensen, J. J. Karlsson, J. Ulstrup, A. V. Xavier, *J. Photochem. Photobiol. A* **1994**, *82*, 103 – 115.
[16] L. Brennan, D. L. Turner, A. C. Messias, M. L. Teodoro, J. LeGall, H. Santos, A. V. Xavier, *J. Mol. Biol.* **2000**, *298*, 61 – 82.

Received: September 28, 2000 [F 138]